UTILIZATION OF LOKPANTA OIL SHALE IN PORTLAND CEMENT MANUFACTURING IN NIGERIA: A THERMODYNAMIC APPROACH

O. A. EHINOLA[*], QINSHAN ZHU

Multiphase Reaction Laboratory, Institute of Process Engineering
CAS, P.O. Box 353, Beijing, 100080, P.R. China

A thermodynamic model is applied to calculate the amount of oil shale ash (OSA), which could be used as raw material in the manufacturing of ordinary Portland cement (OPC). XRF, XRD and SEM analyses of the materials were carried out, and the thermodynamic properties for pure materials in the CaO-SiO_2 system are obtained from literature, database of FACTSAGE and STGE. The main minerals and liquid phase present after blending OSA with cement raw material (employing different blending ratios) at different temperatures indicate that 15 to 20% of OSA would be suitable as clinker material. Temperatures of 1300 and 1400 °C can be used for such a blending ratio due to relatively high amount of C_3S and C_2S. The XRD and SEM of the blend at 1350 °C further show that C_3S and C_2S are the dominant species present. Addition of OSA will definitely lower the clinkering temperature by 50 to 100 °C. Thermomechanical analysis for the suggested blend ratio shows that the liquid is formed at temperatures higher than 1150 °C.

Introduction

Oil shales are rocks that yield oil upon pyrolysis and are considered one of the largest fossil energy potential in the world. An oil shale deposit has been discovered in the Lokpanta area of Abakaliki Fold Belt of the Benue Trough in 1990, and it was named Lokpanta oil shale deposit [1]. Previous studies on the oil shale include: thermal and geochemical characterization of Lokpanta oil shale [2], economic evaluation, recovery techniques and environmental implications of oil shale [3], hydrocarbon potential and depositional environment of oil shale [4, 5].

There is little or no awareness as to the use of oil shale in Nigeria because of the early discovery of crude oil in the Niger Delta Basin. However, oil shale can be utilized in manufacturing of Portland cement, as chemical feed-

---

[*] Corresponding author: e-mail *ehinola01@yahoo.com*

stock, brick, and as asphalt fillers in road construction as well as fossil fuel. In addition to the utilization of spent oil shale after combustion, it can also be used to reduce the temperature required for clinkering reactions.

The principal constituents of ordinary Portland cement (OPC) are calcium silicates (Ca_3SiO_5 and Ca_2SiO_4), aluminate ($Ca_3Al_2O_6$), ferrite ($Ca_4(Al_xFe_{1-x})_4O_{10}$ and they are designated as C_3S, C_2S, C_3A, and C_4AF [6]. Other minerals such as gypsum, anhydrite, calcite, calcium and magnesium oxides, Na and K sulphates are usually also present [6].

Thermodynamic models allow easy and fast parameter variations and make it possible to predict the composition of mineral assemblages under different conditions. The experimental determination of phase diagrams is a time-consuming and costly task and becomes even more pronounced as the number of components increases [7]. The calculation of phase diagrams reduces the effort required to determine equilibrium conditions in a multi-component system. A preliminary phase diagram can be obtained from extrapolation of the thermodynamic functions of constituent subsystems. This preliminary diagram can be used to identify composition and temperature regimes where maximum information can be obtained with minimum experimental effort. This information can then be used to refine the original thermodynamic functions [6].

A thermodynamic cement model has been developed and applied to utilization of oil shale in cement clinkers and to envisage if it can provide the energy source for the clinkering reactions in Jordan [7]. Generally, high percentage of ash in oil shale has been the greatest treat to its usability as fuel. The recent call for alternative source of energy and ban on the importation of cement as well as the policy of government on self-sufficient in cement production in Nigeria have prompted us to examine oil shale as a raw material in the cement industry.

In this study, a comprehensive thermodynamic modeling was conducted to understand the reactions and phases that exist when utilizing the oil shale in production of cement clinker. The results of theoretical thermodynamic equilibrium calculations are compared with experimental values for verifications of these calculations. It is to envisage that the result of this research will therefore create the desired awareness for various stakeholders and policy makers to vibrant ways of engaging and empowering the local cement industry for sustainable development.

Geological setting of Lokpanta oil shale

A northeast-southwest trending belt of Cretaceous sedimentary rocks underlies the study area (Fig. 1). The detailed geology and information on the raw oil shale are already published [2–5]. The Eze-Aku Formation which is the focus of this study consists of black calcareous shales, shelly limestones, siltstones and sandstones that overstep the Asu River Group in most parts of
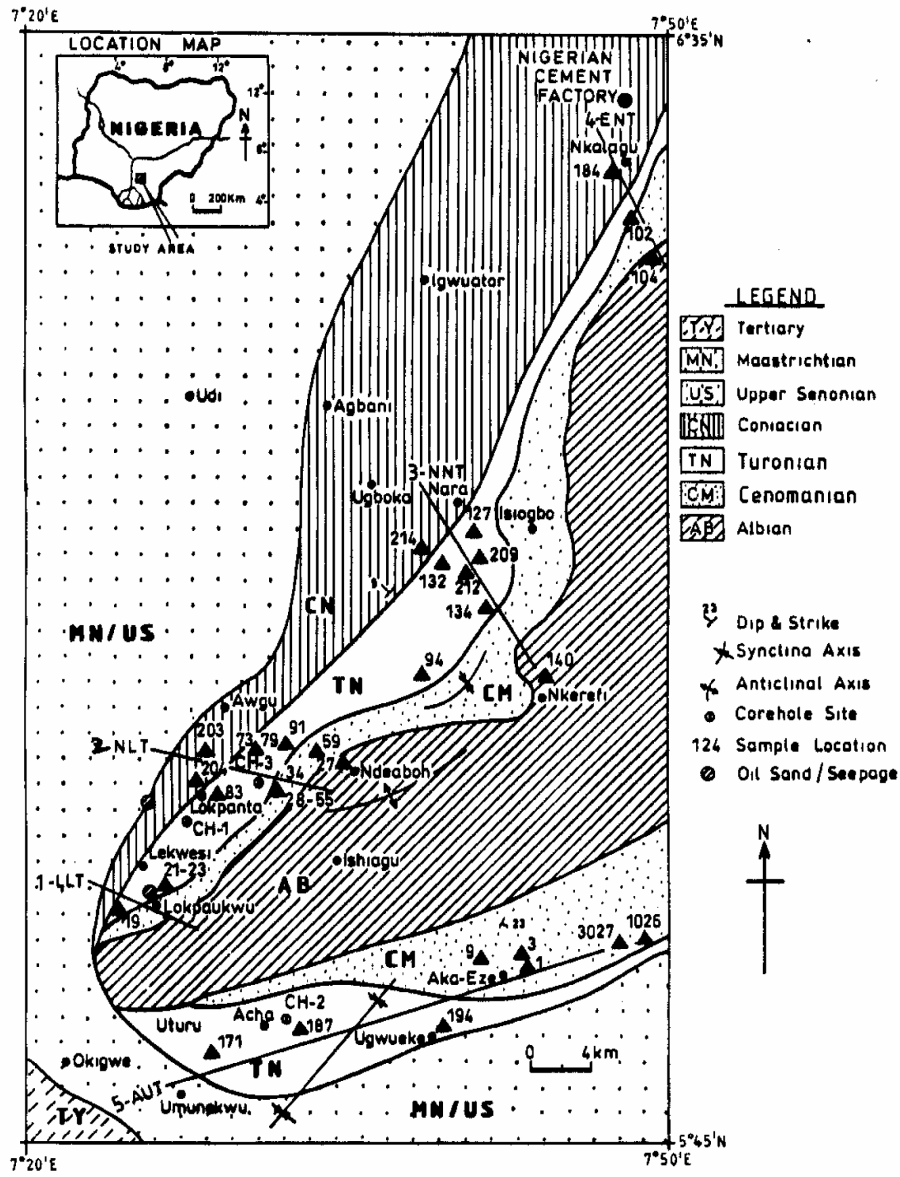
Fig. 1. Geological map ot the lower Benue Trough, SE Nigeria (Modified after Ehinola, 2002).

the Benue Trough [3–5, 8–11]. The Eze-Aku Formation represents the second depositional cycle and has been dated late Cenomania – early Turonian [2, 4, 5, 8, 12].

Materials and methods

The sample materials for this study are oil shale ash (OSA) from Lokpanta and Acha towns, limestones from Nkalagu quarry, clay (kaolinite), and cement raw materials (from Dangote, and Benue cement companies). The materials were crushed to <150 μm while the oil shale was ashed in a SRJX-413 muffle furnace at different temperatures. 50 g of the oil shale sample was heated in air to 500 °C in 30 minutes (at approximately 9 °C per minute), 500 to 815 °C in 60 minutes (at approximately 5 °C per minute and kept at 815 °C for 3 hours (at approximately of 5 °C per minute) and allow to cool at normal temperature [7]. The particle size distribution of sample materials used for this study is presented in Fig. 2. The crystalline component of each material was carried out using automated X'Pert Pro PAnalytical X-ray diffraction (XRD) model. Each sample was put into the sample holder, with two slits of ½ and 1° selected for the incident beam path and 5.0 mm slit for the diffractive path. The compositions of the oil shale ash (OSA), cement raw material, limestones, and clay are presented in Table 1, while the crystalline components are indicated in Fig. 3 and summarized in Table 2. The combination of XRF and XRD results was used to provide an approximate analysis of the main component present in the ash (e.g. anhydrite, quartz, kaolinite, magnetite, lime). Samples of cement raw material from Dangote and Benue cement companies were blended with oil shale ash at different temperatures. Samples of Nkalagu limestone and clay (kaolinite) were also used (Table 3). The scanning electron microscope (SEM) analysis on different materials was carried out using JEOL JSM-6700F model field emission scanning electron microscope. This confirms that the main components present in OSA, limestone and clay are kaolinite, calcite and quartz (Figures 4a-c).
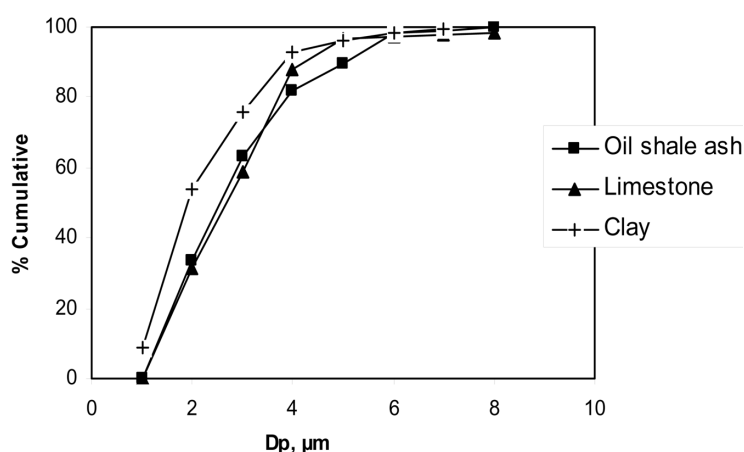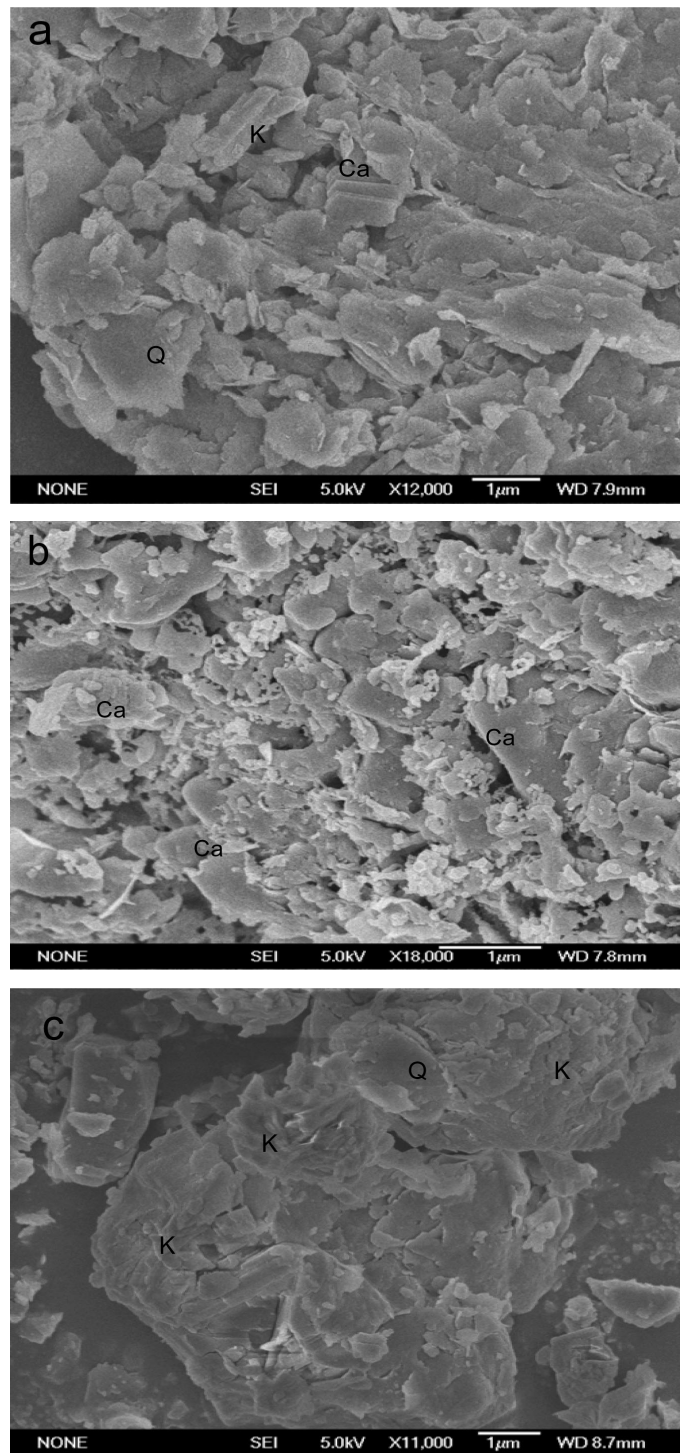

Fig. 2. Particle size distribution of oil shale ash, limestone and clay used for this study.

Fig. 3. X-ray difractograms of kaolinite (a), limestone (b), oil shale ash (c) and cement raw material (d). Q – quartz, K – kaolinite, A – anhydrite, C – calcite, M – magnetite, F – feldspar, C_3S, C_2S, C_3A, and C_4AF.

Fig. 4. Scanning electron photomicrograph of oil shale ash (OSA) (a), limestone (b), clay (c). Ca – calcite, Q – quartz, K – kaolinite.

Table 1. **Chemical compositions of limestone, clay, oil shale ash (OSA), and cement raw material (XRF analysis)**

Oxide	Percentage by weight			
	Limestone	Clay	Oil shale ash	Cement raw material
SiO_2	7.48	60.65	46.86	19.89
CaO	48.29	0.61	19.34	61.38
Fe_2O_3	1.12	0.64	3.21	2.98
Al_2O_3	2.61	25.73	10.03	6.03
MgO	0.77	0.09	0.91	1.78
MnO	0.02	0.01	0.03	0.15
Na_2O	0.04	0.03	0.07	0.11
K_2O	0.20	0.03	1.11	0.88
P_2O_5	0.10	0.03	0.37	0.22
TiO_2	0.12	2.49	0.72	0.33
LOI	38.62	9.54	15.74	4.73
Total	99.37	99.50	98.39	98.63

Table 2. **Crystalline components of limestone, clay, and oil shale ash material (XRD analysis)**

Minerals	Limestone	Clay	Oil shale ash
Quartz	8.64	62.06	35.15
Calcite	91.36	–	35.15
Kaolinite	–	37.94	18.63
Anhydrite	–	–	9.65
Magnetite	–	–	3.08

Table 3. **Composition of blends at 1100, 1200, 1300, 1350 and 1450 °C**

Blend No.	Limestone	Clay	Oil Shale Ash
OSA-1	60	10	25
OSA-2	55	25	20
OSA-3	55	20	25
OSA-3	50	20	30
OSA-4	50	15	35
OSA-5	50	10	40

Thermodynamic calculations

Thermodynamics calculations were performed using a computer program (C++), and mathematical models which are normally used for predictions of multiphase equilibra, liquidus temperatures, and proportions of liquid, and solid phases in a certain atmosphere. The thermodynamic data used for this study are obtained from literature [7, 13–22], phase diagrams, database of sources such as FACTSAGE, H.S.C, CHEMSAGE, THERMOCAL and STGE, as well as experimental data. Gibbs energy functions of all phases of the system and especially the excess Gibbs energy coefficients of the solu-

tion phases are necessary to calculate a temperature-composition phase diagram. The CaO-SiO_2 system has been of great importance in the manufacturing of cement because CaO and SiO_2 are the major components. The thermodynamic properties of pure materials in the CaO-SiO_2 system are summarized in Table 4. A number of different mathematical approaches have been previously used to produce a reasonably calculated phase diagram. In this study, the stoichiometric compound, solid solution of end members and the liquid phases as well as formation energy of mixing were modeled.

The temperature dependence of the Gibbs energies of stoichiometric compound phases is described as polynomial in Eq. (1),

$$G = a + bT + cT \ln T + dT^2 + eT^{-1} + fT^3, \tag{1}$$

where G is the standard Gibbs energy, T is absolute temperature, and a, b, c, d, e and f are constants whose values need to be determined from experimental data. The Gibbs energy is then obtained from the Gibbs-Helmholtz equation

$$G_T = H_T - TS_T, \tag{2}$$

where H_T and S_T are calculated using equations on Table 4.

The end-member (terminal) solid solutions (CaO and SiO_2) are modeled using the

$$G_{ss} = G_{ref} + G_{ideal} + G_{exs}. \tag{3}$$

$$G_{ref} = X_{CaO}G_{CaO} + X_{SiO2}G_{SiO2} \tag{4}$$

$$G_{ideal} = RT(X_{CaO} \ln X_{CaO} + X_{SiO2} \ln X_{SiO2}) \tag{5}$$

$$G_{exs} = X_{CaO}X_{SiO2} \sum L_{CaO,SiO2} (X_{CaOt} - X_{SiO2})^i \tag{6}$$

G_{exs} is the excess Gibbs energy, and expressed by the Redlich-Kister polynomial [14, 18], where L is the binary interaction parameter that has been optimized by several workers [14, 18, 19]. The temperature dependence of L may be expressed as

$$L = a_i + b_i T, \tag{7}$$

where a_i and b_i are considered as enthalpy and entropy terms respectively.

The mole fractions can be obtained from Eq. (8):

$$X_{CaO} = \frac{n_{CaO}}{n_{CaO} + n_{SiO2}}; \quad X_{SiO2} = \frac{n_{SiO2}}{n_{CaO} + n_{SiO2}}, \tag{8}$$

where X_{CaO} and X_{SiO2} are the mole fractions, while n_{CaO} and n_{SiO2} are number of moles of CaO and SiO_2, respectively [21].

Table 4. **Thermodynamic properties of pure materials in the CaO-SiO₂ system**

$H = A + \int_{298.15}^{T} C_p dT\,(J/mol)$, $S = B + \int_{298.15}^{T} (C_p/T) dT\,(J/mole \cdot K)$, $C_p = a + b(10^{-3})T + c(10^5)T^{-2} + dT^{-2/2} + e(10^8)T^{-3} + f(10^{-6})T^2\,(J/mole \cdot K)$

Species	Phases	Temperature range (°K)	A	B	a	b	c	d	e	f
CaO	Lime	298.15–2845	−635090.00	37.749996	58.791171	–	−11.47146	−133.90400	1.02978788	–
CaO	Lime	2845–3500	−657730.78	13.220323	62.760000	–	–	–	–	–
CaO	Liquid	298.15–2845	−555594.00	65.690758	58.791171	–	−11.47146	−133.90400	1.02978788	–
CaO	Liquid	2845–3500	−578234.00	41.161085	62.760000	–	–	–	–	–
SiO₂	Quartz	373–848	−910702.66	41.451419	80.011992	–	−35.46684	−240.27600	4.91568369	–
SiO₂	Quartz	298.15–1996	−908626.77	44.206801	80.011992	–	−35.46684	−240.27600	4.91568369	–
SiO₂	Quartz	1996–3000	−938993.52	2.8387850	85.772000	–	–	–	–	–
SiO₂	Tridymite	298.15–1996	−907045.18	45.523698	75.372668	–	−59.55809	–	9.58246123	–
SiO₂	Tridymite	1996–3000	−936374.98	5.0260850	85.772000	–	–	–	–	–
SiO₂	Cristobalite	298.15–1996	−906377.23	46.028799	83.513598	–	−24.55360	−374.69300	2.80072194	–
SiO₂	Cristobalite	1996–3000	−936216.91	5.1168270	85.772000	–	–	–	–	–
SiO₂	Liquid	298.15–1996	−896795.87	50.829102	83.513598	–	−24.55360	−374.69300	2.80072194	–
SiO₂	Liquid	1996–3000	−926635.55	9.9171310	85.772000	–	–	–	–	–
CaO·SiO₂	Wollastonite	298.15–1813	−1634676.42	79.814260	149.07266	–	−36.593480	−690.29498	4.8434942	–
CaO·SiO₂	Wollastonite	1813–1815	−1673238.73	23.073612	146.44000	–	–	–	–	–
CaO·SiO₂	Pseudowollastonite	298.15–1813	−1625506.56	86.936460	141.15611	–	−58.575950	−417.23200	9.40734953	–
CaO·SiO₂	Pseudowollastonite	1813–1815	−1665900.39	28.391783	146.44000	–	–	–	–	–
2CaO·SiO₂	Gamma (Olivine)	298.15–1120	−2325867.11	109.694627	255.22000	–	–	−2340.8000	1.41040000	–
2CaO·SiO₂	Alpha-Prime	298.15–1710	−2304009.14	123.414327	230.83672	–	−79.894003	−1033.0877	12.9747995	–
2CaO·SiO₂	Alpha-Prime	1710–2500	−2290092.43	138.024936	209.68000	–	−79.893999	−701.90002	12.9747995	–
2CaO·SiO₂	Alpha	298.15–2500	−2278595.98	144.748016	209.68000	–	−79.893999	−701.90002	12.9747995	–
3CaO·SiO₂	Hatrurite	298.15–2500	−2929057.11	169.905571	268.90967	–	−80.108946	−545.93735	0.97508363	–
3CaO·2SiO₂	Rankinite	298.15–5000	−3948801.63	206.183102	392.84876	–	−10.659996	−2200.0658	13.7358913	–

The association model was used to describe the Gibbs energy of the liquid phase [14]. The association–species solution model uses intermediate "Chemical species" with their corresponding thermodynamic data, to represent the negative, non-ideal mixing of the end-member components in a system. For example, a liquid $CaSiO_3$ (l) species is ideally mixed with end-member CaO (l) and SiO_2 (l) to represent the liquid phase in the CaO-SiO_2 binary system. While $CaSiO_3$ (l) may not exist as a chemical entity that can be isolated and characterized, this species in the model can accurately represent the negative interaction energy that occurs between calcium and silica in oxide liquid solution [14].

The associate species for the modeling of the liquid phase include $CaSiO_3$ (wollastonite) which is stable between 298 to 1398 K, $CaSiO_3$ (pseudo-wollastonite) which is stable at 1398 to 1817 K, Ca_2SiO_4 (calcium othosilicate), Ca_3SiO_5 which is stable in the temperature range from 1523 to 2343 K and $Ca_3Si_2O_7$ (rankinite) which is stable up to 1737 K [17]. Based on Besmann and Spear [14] equation:

$$G_{exs} = X_{SiO2}\left(1 - X_{SiO2}\right)\left[\left(141000 - 65T\right) + \left(-10000 - 10T\right)\left(1 - 2X_{SiO2}\right)\right]. \quad (9)$$

Chemical reactions and associated equilibrium constants can be used in determining the relative amounts of each species [14].

$$CaO_{(l)} + SiO_{2(l)} = CaSiO_{3(l)} Keq = \left(\gamma_{CaSiO3(l)}\right) / \gamma_{CaO}\gamma_{SiO2(l)}. \quad (10)$$
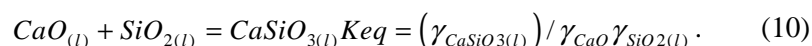
However, the Gibbs energy of formation of the main species were calculated using

$$G_f = G_p - G_{r1} - G_{r2}, \quad (11)$$

where G_f is standard Gibbs energy of formation, G_p is the product and G_{r1} and G_{r2} are reactants.

C++ computer program language was adopted for the above mathematical models to calculate the quantities of minerals that are noted to be the most important constituents in Portland cement such as tricalcium silicate (C_3S), calcium othosilicate (C_2S), tricalcium aluminate (C_3A) and tetracalcium aluminoferate (C_4AF) at different temperatures.

Thermomechanic analysis

Thermomechanic analysis was carried out using a 50 mg sample of oil shale ash compressed to 0.35 MPa. The ash pellet was sintered in an oven to 1450 °C and sintering occurred at 1050 °C. This was used to verify the results obtained from the computer program calculations. Scanning electron microscopic (SEM) images were obtained for the suggested blend at appropriate temperature.

Results and discussion

The thermodynamic properties for a pure CaO-SiO$_2$ system which includes CaO, Al$_2$O$_3$, SiO$_2$ and intermediate compounds such as CaSiO$_3$, Ca$_2$SiO$_4$, Ca$_3$SiO$_5$, Ca$_3$Si$_2$O$_7$, and Ca$_3$Al$_2$O$_6$ are presented in Table 4. The free energy (*G*), enthalpy of mixing (*H*), entropy (*S*) and heat capacity (*Cp*) are calculated using Table 4 equations, and a typical result of calculated thermodynamic functions for the CaO-SiO$_2$ system at different temperatures is shown in Table 5. The results coincide excellently with those of the database of Viewdata of Factsage 5.1 [22]. Computation of crystalline, solid solution and liquid phases were performed using equations (1) to (11). Figure 5 shows the results of thermodynamic calculations for oil shale ash (OSA), C$_3$S$_2$ occurring in large proportions. C$_3$S and C$_2$S which are important constituents of Portland cement are formed below 1300 °C. The low quantity of lime in OSA would possibly affect its cementing properties, as it is noted that the amount of lime to form CaO should be from 65 to 75% (Fig. 6). C$_2$S starts to precipitate out of the liquid slag above 1450 °C, and this is slightly different from the data reported for the Jordanian oil shale [7]. This may be attributed to the mineral composition of the Lokpanta oil shale.

Table 5. **A typical result of calculated thermodynamic functions for the CaO-SiO$_2$ system**

CaO·SiO$_2$ (wollastonite)			
T (K)	*C$_p$* (J/mol·K)	*H* (J/mol)	*S* (J/mol·K)	*G^0*
298.15	86.204312	−1634676.420000	79.814260	−1658473.041619
498.15	107.316273	−1613213.165438	134.900188	−1680413.694091
698.15	116.863081	−1587931.187490	179.245724	−1713071.589919
898.15	122.171315	−1561373.631277	214.537501	−1754060.488168
1098.15	125.573248	−1534217.821997	243.534840	−1801655.607024
1298.15	127.963617	−1506712.802529	268.061376	−1854696.677910
1498.15	129.751966	−1478974.060548	289.284482	−1912365.607024
1698.15	131.151368	−1451064.505497	307.978030	−1974057.397118
1813.00	146.440000	−1451404.096000	287.418533	−1972493.895522
2CaO·SiO$_2$ (alpha)			
T (K)	*C$_p$* (J/mol·K)	*H* (J/mol)	*S* (J/mol·K)	*G^0*
298.15	128.108993	−2278595.980000	144.748016	−2321752.600970
498.15	156.532353	−2247289.509460	225.096780	−2359421.470572
698.15	170.537014	−2210381.174272	289.847263	−2412738.040687
898.15	178.145946	−2171708.412521	341.196743	−2478154.267576
1098.15	182.853775	−2132312.960125	383.150118	−2553069.262143
1298.15	186.051088	−2092544.892408	418.447536	−2635752.561335
1498.15	188.372078	−2052549.486054	448.853936	−2725000.009954
1698.15	190.141584	−2012397.762519	475.536947	−2819930.828574
1898.15	191.541736	−1972129.202454	499.299104	−2919873.795962
2098.15	192.682156	−1931768.099806	520.712245	−3024300.496708
2298.15	193.632664	−1891330.651621	540.196845	−3132784.029908
2498.15	194.439828	−1850828.358366	558.070513	−3244972.209224

Continued

| 3CaO·SiO₂ (hatrurite)				
T (K)	C_p (J/mol·K)	H (J/mol)	S (J/mol·K)	G^0
298.15	150.853422	−2929057.110000	169.905571	−2979714.455994
498.15	212.956083	−2886465.893485	279.216891	−3025557.787708
698.15	232.098880	−2836217.557910	367.383947	−3092706.660638
898.15	240.896833	−2784519.010382	435.552235	−3175710.250266
1098.15	245.865911	−2732364.381225	490.461983	−3270965.207774
1298.15	249.048185	−2680008.925000	536.280042	−3376180.860887
1498.15	251.264730	−2627539.434037	575.544732	−3489791.774479
1698.15	252.903467	−2574992.256128	609.881223	−3610662.055712
1898.15	254.169752	−2522385.506982	640.383514	−3737929.474394
2098.15	255.181912	−2469729.668497	667.820235	−3870916.694458
2298.15	256.012756	−2417031.597885	692.750954	−4009077.202887
2498.15	256.709493	−2364296.225386	715.595256	−4151960.514538
3CaO·2SiO₂ (rankinite)				
T (K)	C_p (J/mol·K)	H (J/mol)	S (J/mol·K)	G^0
298.15	305.269112	−3948801.630000	206.183102	−4010275.121861
498.15	301.092166	−3888583.196748	360.735072	−4068283.372942
698.15	311.433486	−3824228.235579	471.162317	−4153170.207287
898.15	320.012146	−3756794.342669	559.073416	−4258926.131175
1098.15	326.611689	−3687512.279124	632.014689	−4381559.209545
1298.15	331.781770	−3617019.860256	694.266845	−4518282.364534
1498.15	335.941793	−3545671.477946	748.524032	−4667072.756053
1698.15	339.371104	−3473682.084017	796.586329	−4826405.158308
1898.15	342.256179	−3401191.743607	839.712395	−4995091.825540
2098.15	344.724790	−3328297.007989	878.815134	−5172182.981468
2298.15	346.867087	−3255067.456144	914.576925	−5356902.415656
2498.15	348.748447	−3181555.046645	947.520822	−5548604.187942
2698.15	350.417462	−3107799.721279	978.056377	−5746742.533838
2898.15	351.911039	−3033832.929471	1006.510154	−5950850.331484
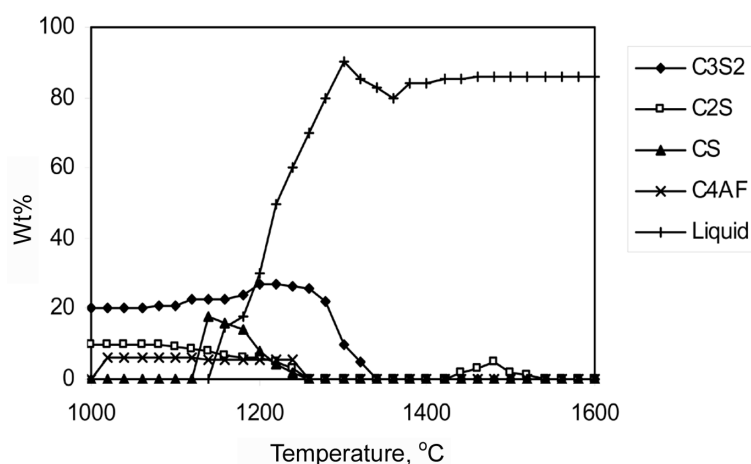
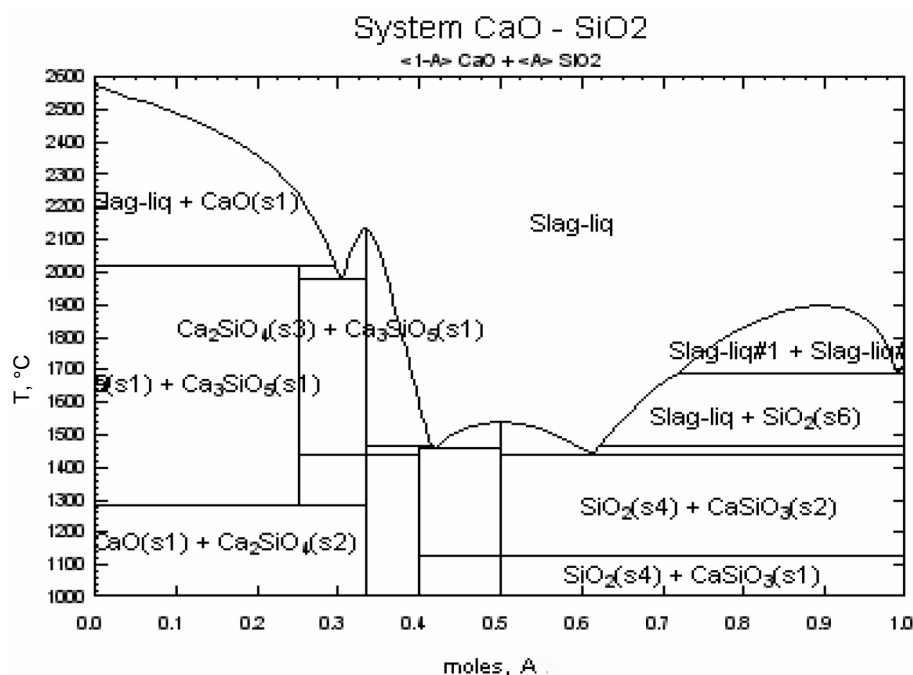*Fig. 5.* Thermodynamic equilibrium diagram for oil shale ash (OSA).

Fig. 6. Phase diagram of the CaO-SiO$_2$ system [17, 22].

Main clinker minerals and liquid phase present after blending OSA with cement raw material at 1250, 1300, 1350, 1450 °C were computed and the results plotted as shown in Fig. 7. The results of the thermodynamic modelling (e.g. Fig. 7) show that even at the lowest level of OSA addition (15%), the clinker minerals are very significantly altered. At 1250 °C, neither the OSA blends nor the cement raw material would be a suitable clinker material due to low amount of C$_3$S which is reported to be stable at temperatures between 1300 and 1800 °C. C$_3$S and C$_2$S are noted to be in equilibrium at above 1250 and below 1420 °C [7]. The OSA blending ratio of 15 to 20% could be used in making clinker materials at temperatures between 1300 and 1350 °C due to relatively high amounts of C$_3$S and C$_2$S. At this blending ratio, there are enough liquids (>20%) to proceed to clinkering reactions during the process of making cement. The minimum amount of liquid required for clinkering reactions is about 20% [7].

Table 3 shows the different blending ratios employed in the mathematical computation of the raw materials which are considered in the manufacturing of cement. The optimum blending ratio obtained for the constituents that is close to Portland cement is 20% OSA, 15% clay and 65% limestone (Fig. 8). The constituents present at different ratios indicate that a temperature between 1300 and 1400 °C can be used for the blending ratio that makes up all necessary components of cement clinkers (Fig. 9). This is an indication that the addition of OSA will reduce the required temperature to about
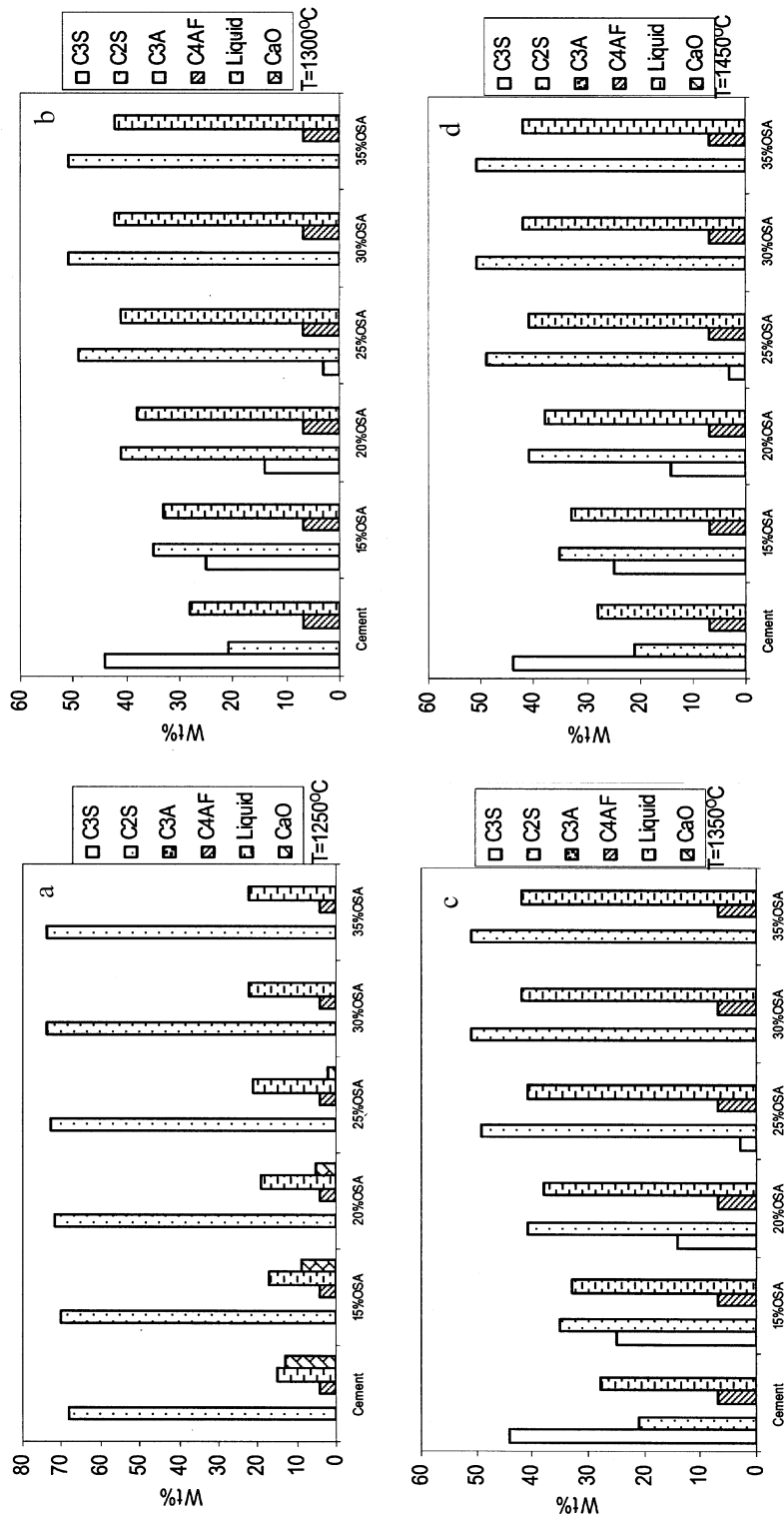
Fig. 7. Clinker minerals and liquid phase determined after blending OSA with ordinary Portland cement at 1250 °C (a), 1300 °C (b), 1350 °C (c) and 1450 °C (d).
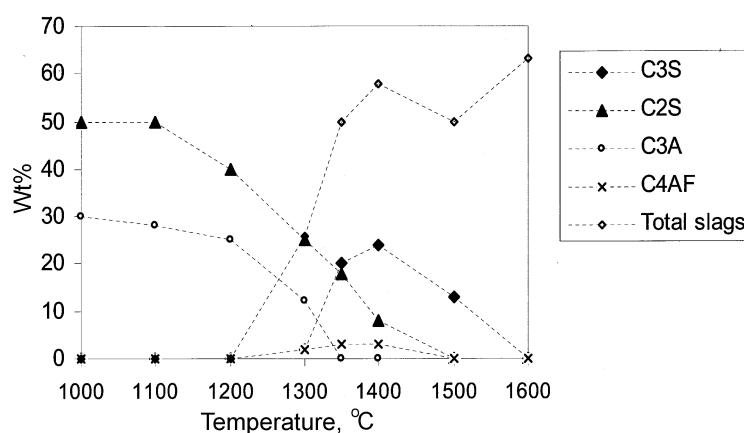
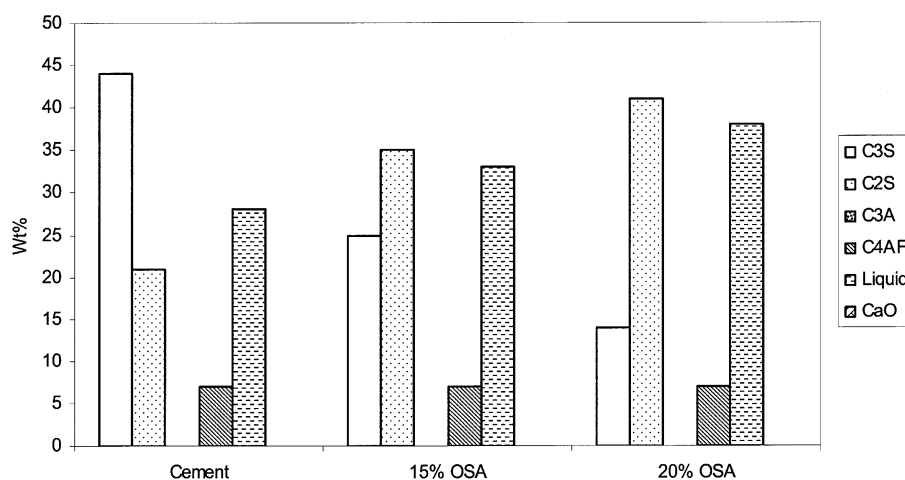*Fig. 8.* Calculation for the main constituents present when blending 25% OSA, 15% clay and 60% lime.

Fig. 9. Percentage of cement components present when blending 20% OSA, 15% clay and 65% limestone.

1350–1400 °C instead of 1450–1500 °C. At this temperature, there will be enough liquid constituents to undergo the clinkering reactions [7].

Thermomechanical analysis result for the suggested blend ratio shows that the liquid has formed at temperatures higher than 1150 °C. Sintering occurred at this temperature when OSA was not blended, and that resulted in the shrinkage of the pellet. The XRD and SEM of the blend at 1350 °C show that C_3S and C_2S are the dominant components present (Fig. 10).
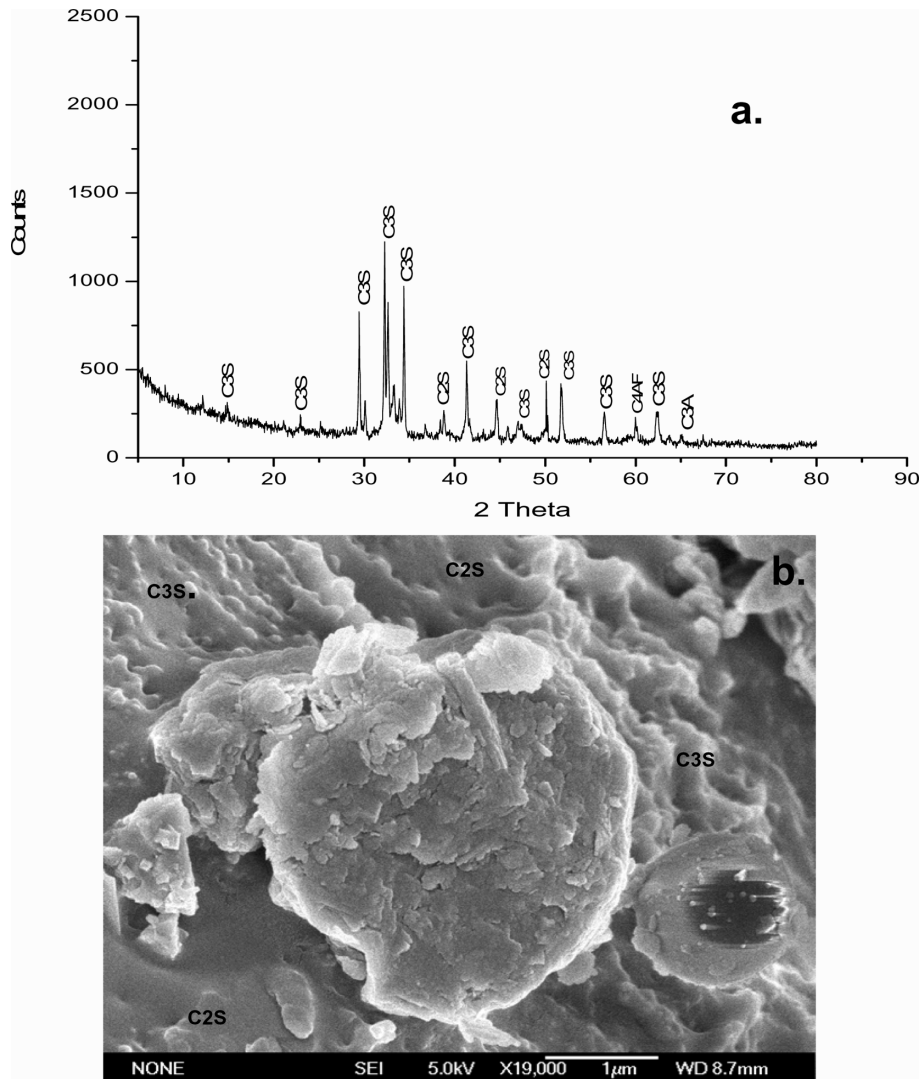
Fig. 10. XRD of the suggested blend ratio (a) and SEM of the suggested blend ratio at temperature > 1350 °C (b).

Conclusions

Huge amounts of oil shale ash (OSA) and the cost of its disposal have been the greatest challenge to usability of oil shale as a source of energy. An attempt has been made on utilization of Lokpanta oil shale as raw material in the cement manufacturing in Nigeria using a thermodynamic model. From the different blending ratios employed in the thermodynamic calculation, the optimum ratio obtained for the constituents that is close to Portland cement was 20% OSA, 15% clay and 65% of limestone. Temperature between 1300

and 1400 °C is suggested for the blending ratio that makes up all necessary components of cement clinkers indicating a reduction in the required clinkering temperature. More experiments should be carried out on the suggested blending ratio to ascertain the geotechnical engineering properties and applications.

Acknowledgements

REFERENCES

1. *Ekweozor, C. M., Unomah, G. I.* First discovery of oil shale in the Benue Trough, Nigeria // Fuel. 1990. Vol. 69, No. 4. P. 502–508.
2. *Sonibare, O. O., Ehinola, O. A., Egashira, E.* Thermal and geochemical characterization of Lokpanta oil shale, Nigeria // Energy Convers. Manage. 2005. Vol. 46, No. 15–16. P. 2335–2344
3. *Ehinola, O. A., Sonibare, O. O., Akanbi, O. A.* Economic evaluation, recovery techniques, and environmental implications of the oil shale deposits in the Abakaliki anticlinorium, Southeastern Nigeria // Oil Shale. 2005. Vol. 22, No. 1. P. 5–19
4. *Ehinola, O. A.* Depositional Environment and Hydrocarbon Potential of the Oil Shale Deposit from the Abakaliki Fold Belt, Southeastern Nigeria, Ph.D thesis, University of Ibadan, 2002, 240 p.
5. *Ehinola, O. A., Bassey, C. E., Ekweozor, C. M.* Preliminary studies of the lithostratigraphy and depositional environment of the oil shale deposits of Abakaliki anticlinorium, southeastern, Nigeria // Journal of Mining and Geology. 2003. Vol. 39, No. 2. P. 85–94.
6. *Lobthenbach, B., Winnefeld, F.* Thermodynamic modeling of the hydration of Portland cement // Cement Concr. Res. 2006. Vol. 36, No. 2. P. 209–226.
7. *Al-Otoom, A. Y.* A thermodynamic study on the utilization of Jordanian oil shale in the cement industry // Oil Shale. 2005. Vol. 22, No. 1. P. 37–49.
8. *Ojoh, K. A.* Cretaceous geodynamic evolution of the southern part of of the Benue trough (Nigeria) in the equatorial domain of the South Atlantic. Stratigraphy, basin analysis and paleo-oceanography // Bulletin des Centres de Recharches Exploration-Production Elf-Aquitaine. 1990. Vol. 14, No. 2. P. 419–442.

9. *Reyment, R. A*. Aspects of the Geology of Nigeria. – Ibadan, Nigeria: Ibadan Univ. Press, 1965. 145 p.

10. *Benkhelil, J.* The origin and evolution of the Cretaceous Benue trough (Nigeria) // J. Afric. Earth Sci. 1989. Vol. 8, No. 2–4. P. 251–282.

11. *Akande, S. O., Erdtmann, B. D*. Burial metamorphism (thermal maturation) in Cretaceous sediments of the southern Benue Trough and Anambra basin, Nigeria // Am. Assoc. Petrol. Geol. Bull. 1998. Vol. 82, No. 6. P. 1191–1206.

12. *Amajor, L. C*. The Cenomanian hiatus in the Southern Benue Trough, Nigeria // Geological Magazine. 1985. Vol. 122, No. 1. P. 39–50.

13. *Eriksson, G., Wu, P., Pelton, A. D*. Critical evaluation and optimization of the thermodynamic properties and phase diagrams of the $MgO–Al_2O_3$, $MnO–Al_2O_3$, $FeO–Al_2O_3$, $Na_2O–Al_2O_3$ and $K_2O–Al_2O_3$ // Calphad. 1993. Vol. 17, No. 2. P. 189–205.

14. *Besmann, T. M., Spear, K. E*. Thermodynamical modeling of oxide glasses // J. Am. Ceram. Soc. 2002. Vol. 85, No. 12. P. 2887–2894.

15. Pelton, A. D., Wu, P. Thermodynamic modeling in glass-forming melts // J. Non-Cryst., Solids. 1999, Vol. 253, No. 1. P. 178–191.

16. *Eriksson, G., Hack, K*. SGTE Pure Substance Database, 1996 Version, produced by the Scientific Group Thermodata Europe, and obtained through GTT Technologies. – Germany: Herzogonrah, 1996.

17. *Lee, Y. E*. Thermodynamics of $CaO-SiO_2$ system // Calphad. 1982. Vol. 6, No. 4. P. 283–291.

18. *Chatterjee, N. D*. Applied Mineralogical Thermodynamics: Selected Topics. – Springer-Verlag, 1991. P. 33–164.

19. *Bale, C. W., Eriksson, G*. Metallurgical thermodynamical databases: A review // Canad. Metall. Quarterly. 1990. Vol. 29, No. 2. P. 105–132.

20. *Saunders, N., Miodownik, A. P*. Calphad (Calculation of Phase Diagrams), A Comprehensive Guide: Pergamon Materials series. – Elsevier Science Ltd, 1998. P. 30–408.

21. *Smith, B. E*. Basic Chemical Thermodynamics, fifth edition. – London: Imperial College Press, 2004. P. 104–240.

22. *Jak, E., Degterov, S. A., Pelton, A. D., Happ, J., Hayes, P.C*. Thermodynamic modeling of the system Al_2O_3-SiO_2-CaO-FeO-Fe_2O_3 to characterise coal ash slags // Impact of Mineral Impurities in Solid Fuel Combustion / R. P. Gupta, T. F. Wall, L. Baxter (Eds.). NY: Kluwer Academic Plenum Publ., 1999. P. 723–733.